IEEE Access
Multidisciplinary ⋮ Rapid Review ⋮ Open Access Journal

Received May 25, 2020, accepted June 23, 2020, date of publication June 29, 2020, date of current version July 7, 2020.

Digital Object Identifier 10.1109/ACCESS.2020.3005408

Channel Sparsity Aware Function Expansion Filters Using the RLS Algorithm for Nonlinear Acoustic Echo Cancellation

JEAN JIANG[1], (Senior Member, IEEE), VINITH VIJAYARAJAN[2], AND LIZHE TAN[3], (Senior Member, IEEE)

[1]College of Technology, Purdue University Northwest, Hammond, IN 46323, USA
[2]Qualcomm Inc., San Diego, CA 92121, USA
[3]Department of Electrical and Computer Engineering, Purdue University Northwest, Hammond, IN 46323, USA

Corresponding author: Jean Jiang (jjiang@pnw.edu)

This work was supported in part by the Purdue University Northwest Exploratory Grant 2017-2018.

ABSTRACT In this paper, we propose a channel sparsity aware sequential recursive least squares (sparse SEQ-RLS) algorithm for function expansion filters with applications in nonlinear echo cancellation. The algorithm is developed based on a diagonal channel structure from the Volterra filter and updating dominant coefficients taking into consideration of sparse elements in the diagonal channel. The third-order Volterra, third-order even mirror Fourier nonlinear (EMFN), and functional link artificial neural network (FLANN) filters are developed according to the sparse SEQ-RLS algorithm. The computation complexity for the upper bound is analyzed to validate the efficiency for each proposed filter. Computer simulation results demonstrate that all proposed function expansion filters with the sparse SEQ-RLS algorithm are effective for nonlinear echo cancellation. In general, the EMFN filter provides better performance compared to the Volterra and FLANN filters.

INDEX TERMS Nonlinear sparse system modeling, nonlinear acoustic echo cancellation, sparse sequential RLS algorithm, Volterra filter, even mirror Fourier nonlinear filter.

I. INTRODUCTION

Speech quality is in demand for voice commanded systems and telephony [1]–[4]. The voice communication system in real time often suffers from audible echoes. In order to cancel the echoes, an acoustic echo cancellation system is designed to increase speech quality both subjectively and objectively. Although echo cancellation has been studied for several decades, some fundamental challenges still need to be addressed. One of them is the non-linearity in the acoustic echo path in which nonlinearities may be introduced by low quality and overdriven audio components such as amplifiers, loudspeakers, and so on. A conventional linear echo canceller cannot model the nonlinear echo path accurately; thus the echo cancellation system suffers from performance degradation.

In order to tackle the problems of nonlinear acoustic echo cancellation (NAEC), several nonlinear filters have been investigated [2]–[6], including the linear FIR filter with non-linear preprocessor, static power filter, cascade and parallel dynamic power filter, hybrid Taylor-Volterra model filter and functional link neural network. Most of the proposed nonlinear filters use the least mean squares (LMS) algorithm and its variations. To improve effectiveness of nonlinear echo cancellation and algorithm convergence speed, the recursive least squares (RLS) algorithm [6] has been applied. However, the RLS algorithm suffers when the dimension of the input vector is large, resulting in algorithm instability, and a huge computational load, which hinders its real-time implementation. Recently, the diagonal Volterra structure and functional link artificial neural network (FLANN) filters [7], [8] have been introduced to improve the processing capability using a sequential RLS algorithm [9]–[13] in which the filter channel can be updated sequentially. But the even mirror Fourier (EMFN) nonlinear filter [14], [15] using the RLS algorithm has not been reported yet for nonlinear acoustic echo cancellation.

On the other hand, although an improvement using the nonlinear filters for NAEC has been validated, many of the filter coefficients during the adaptive process for modeling

The associate editor coordinating the review of this manuscript and approving it for publication was Junhua Li.

the nonlinear echo path are not significant and their values are close to zero. Such sparsity in the nonlinear filter coefficients can be exploited by updating the significant filter coefficients [16]–[20] and setting the non-significant coefficients to zero.

In this paper, we develop function expansion adaptive filters wielding a new channel sparsity-aware recursive least squares (RLS) algorithm using a sequential update. The developed nonlinear adaptive filters using a sparse sequential RLS (SEQ-RLS) algorithm adopt a discard function to neglect the coefficients whose values are close to zero in the weight vector for each filter channel in order to reduce the computational load and to improve the algorithm convergence rate. Therefore, the channel sparsity-aware algorithm is first derived for nonlinear system modeling and then modified for echo cancellation. The proposed channel sparsity-aware algorithm requires less computational load in comparison with the non-sequential sparsity-aware algorithm.

To evaluate the performance of the proposed functional expansion adaptive filters using the sparse SEQ-RLS algorithm, several simulation experiments are conducted, including nonlinear system identification and nonlinear AEC in single-talk and double-talk scenarios.

The structure of this paper is organized as follows.

Section II proposes a new channel sparsity aware sequential RLS algorithm. In Section III, we introduce popular polynomial expansion filters for effectively modelling a nonlinear echo path. Analysis of algorithm computational complexity is included. Section IV presents the simulation results and discussion. Finally, the conclusion is presented in Section V.

This paper presents the following contributions:

a. Develops a framework of the sequential RLS algorithm for function expansion filters using the diagonal structure, particularly, for the even mirror Fourier nonlinear (EMFN) filter. The proposed filters have a significant advantage over the standard RLS algorithm which is not feasible for real-time applications due to a huge computational load with a large filter size for the application of echo cancellation.

b. Develops a framework for the sequential RLS algorithm by consideration of the filter coefficient sparsity using a discard function;

c. Validates the performances of the function expansion filters for applications of nonlinear system identification and acoustic echo cancelation; validates the advantage of the new sparse SEQ-RLS EMFN filter.

II. SPARSE SEQUENTIAL RLS ALGORITHM

A standard nonlinear echo cancellation system is described in Fig. 1.

As shown in Fig. 1, $x(n)$ is the speech signal from the far end, which passes through a digital to analog conversion (DAC) unit. The converted analog speech signal drives the amplifier and speaker, and nonlinear distortion may occur due to saturation of the speaker amplifier. A portion of distorted speech signal (echo signal) from the far end is further leaked through the acoustic channel, microphone, and the

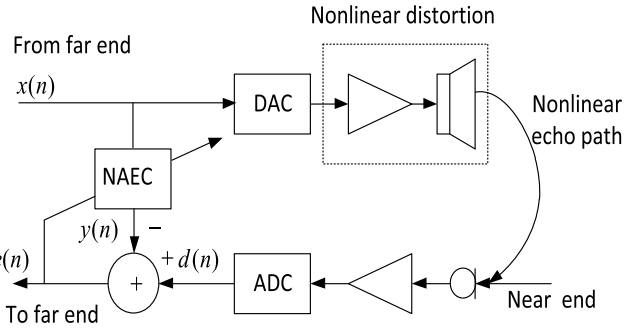

FIGURE 1. Echo cancellation system.

analog to digital conversion (ADC) unit. The output $d(n)$ from the ADC contains the near-end speech and echo signal. This echo signal can be cancelled by a nonlinear echo canceller whose output $y(n)$ is generated by an adaptive filter, that is, the nonlinear acoustic echo canceller (NAEC). For our framework, a multichannel adaptive filter is adopted, that is,

$$y(n) = \sum_{k=0}^{M} W_k^T(n) X_k(n). \tag{1}$$

The filter has $M+1$ channel sub filters. As depicted in Fig. 1, the error due to the far end at past time index i is expressed as

$$e(i) = d(i) - \sum_{k=0}^{M} W_k^T(n) X_k(i) \quad \text{for } 1 \le i \le n \tag{2}$$

where the kth channel sub filter with a size of M_k has its weight vector and input vector defined below:

$$W_k(n) = [\, w_0(n) \quad w_1(n) \quad \dots \quad w_{M_k}(n) \,]^T \tag{3}$$

$$X_k(i) = [\, x(i) \quad x(i-1) \quad \dots \quad x(i-M_k) \,]^T. \tag{4}$$

For the sequential RLS (SEQ-RLS) algorithm developed in [10], the following objective function is minimized:

$$\zeta(n) = \frac{1}{2} \sum_{i=1}^{n} \lambda^{n-i} \left(d(i) - \sum_{k=0}^{M} W_k^T(n) X_k(i) \right)^2 \tag{5}$$

where $0 \ll \lambda < 1$. The SEQ-RLS algorithm has significant reduction of the computational load in comparison with the standard RLS algorithm. Considering that an adaptive filter for echo cancellation as shown in Fig. 1, may have many non-significant filter coefficients with values close to zero, a sparse algorithm can be developed to further reduce the computational load as well as the steady-state error. Similar to [19], a discard function can be employed in the adaptive algorithm, that is,

$$f(w) = \begin{cases} w & |w| > \varepsilon \\ 0 & |w| \le \varepsilon \end{cases} \tag{6}$$

where ε is the small threshold value and w is designated as the element of the adaptive filter coefficients. Using (6), the

TABLE 1. Sparse SEQ-RLS algorithm.

For $j = 0,1,...,M$

$Q_j(-1) = \delta I / E\{x_j^2(n)\}$; $W_j(-1) = 2\varepsilon[1...1]$; $\delta =$ small value

For $n = 0,1,...$

$$\alpha(n) = d(n) - \sum_{k=0}^{M} X_k^T(n) f(W_k(n-1))$$

For $j = 0,1,...,M$

$$k_j(n) = \frac{\lambda^{-1} Q_j(n-1) F(W_j(n-1)) X_j(n)}{1 + \lambda^{-1} X_j^T(n) F(W_j(n-1)) Q_j(n-1) F(W_j(n-1)) X_j(n)}$$

$$Q_j(n) = \lambda^{-1} Q(n-1) - \lambda^{-1} k_j(n) X_j^T(n) F(W_j(n-1)) Q_j(n-1)$$

$$W_j(n) = W_j(n-1) + k_j(n)\alpha(n)$$

end

$$y(n) = \sum_{k=0}^{M} f^T(W_k(n)) X_k(n)$$

objective function expressed in (5) can be changed to

$$\zeta(n) = \frac{1}{2} \sum_{i=1}^{n} \lambda^{n-i} \left(d(i) - \sum_{k=0}^{M} f^T(W_k(n)) X_k(i) \right)^2 . \quad (7)$$

Minimizing Equation (7) leads to a sparse SEQ-RLS algorithm [9], [10], which is listed in Table 1.

Note that $F(W_j(n))$ denotes the Jacobian matrix of $f(W_j(n))$. It is essentially a diagonal matrix with elements of either ones or zeros. This framework can be further applied to the different function expansion filters such as the FLANN, Volterra, and EMFN filters.

III. FUNCTION EXPANSION FILTERS

In order to model a nonlinear echo path due to signal companding and/or due to over driven amplifiers to near saturation, we apply the sparse SEQ-RLS algorithm to the following functional expansion filters.

A. VOLTERRA FILTERS

Let $x(n)$ and $y(n)$ be the input and output signals respectively. The second-order Volterra series expansion [2], [3], [7] with a memory length of $N + 1$ in terms of the diagonal channel based-structure is given by

$$y(n) = f^T(W_0(n)) X_0(n) + \sum_{k=1}^{N_2} f^T(W_k(n)) X_k(n) \quad (8)$$

where N_2 is the number of significant second-order channels, $W_0(n)$ and $X_0(n)$ are the linear filter coefficient vector and corresponding linear input vector while $W_k(n)$ and $X_k(n)$ are the filter coefficient vector and corresponding input vector of the kth second-order Volterra diagonal channels. By selecting $N_2 \ll N + 1$, we can achieve a great deal of computational load reduction. The third-order Volterra filter based on the diagonal channel structure can be developed similarly, that

TABLE 2. Channel input vectors in the Volterra filter.

Input vector	Elements
$X_0(n)$	$x(n), x(n-1), \cdots, x(n-N)$
$X_1(n)$	$x^2(n), x^2(n-1), \cdots, x^2(n-N)$
$X_2(n)$	$x(n)x(n-1), x(n-1)x(n-2), ..., x(n-N+1)x(n-N)$
...	...
$X_{N_2}(n)$	$x(n)x(n-N_2+1), x(n-1)x(n-N_2), \cdots$
$X_{N_2+1}(n)$	$x^3(n), x^3(n-1), \cdots, x^3(n-N)$
$X_{N_2+2}(n)$	$x^2(n)x(n-1), x^2(n-1)x(n-2), \cdots, x^2(n-N+1)x(n-N)$
...	...
$X_{N_2+1+P_3}(n)$	$x^2(n)x(n-P_3), x^2(n-1)x(n-P_3-1), \cdots$
$X_{N_2+2+P_3}(n)$	$x(n)x^2(n-1), x(n-1)x^2(n-2), \cdots, x(n-N+1)x^2(n-N)$
...	...
$X_{N_2+1+2P_3}(n)$	$x(n)x^2(n-P_3), x(n-1)x^2(n-P_3-1), \cdots$
$X_{N_2+2+2P_3}(n)$	$x(n)x(n-1)x(n-2), x(n-1)x(n-2)x(n-3),$
...	$\cdots, x(x-N+2)x(n-N+1)x(n-N)$
	...
$X_{N_2+N_3}(n)$	$x(n)x(n-P_3+1)x(n-P_3), x(n-1)x(n-P_3)x(n-P_3-1), ...$

is,

$$y(n) = f^T(W_0(n)) X_0(n) + \sum_{k=1}^{N_2} f^T(W_k(n)) X_k(n) + \sum_{k=N_2+1}^{N_2+N_3} f^T(W_k(n)) X_k(n) \quad (9)$$

where $W_{N_2+1}(n), \ldots, W_{N_2+N_3}(n)$ and $X_{N_2+1}(n), \ldots, X_{N_2+N_3}(n)$ designate the third-order diagonal channel coefficient vectors and the corresponding input vectors.

Note that $N_3 = 1 + 2P_3 + (P_3 - 1)P_3/2 = (P_3 + 1)(P_3 + 2)/2$ is the total number of the third-order Volterra diagonal channels and P_3 is the maximum delay in the first element in the invariant third-order diagonal channels as shown in Table 2. Since $N_3 \ll (N + 1)(N + 3)N/2$ (total number of third-order diagonal channels), a significant reduction of the computational load can be obtained. The signal vectors for time-invariant channels are listed in Table 2.

B. FUNCTIONAL LINK ARTIFICIAL NEURAL NETWORK (FLANN) FILTER

Although the digital Volterra filter has the property of being a universal approximation for causal, time invariant, finite-memory nonlinear systems, modeling the nonlinear echo path will require a large number of filter coefficients in order to compensate the nonlinear behavior as well as the echo response time.

An alternative choice is the functional link artificial neural network (FLANN) adaptive filter [8]. The relationship between the input and output for a FLANN filter with an order

TABLE 3. Channel input vectors in the FLANN filter ($P = 2$).

Input vector	Elements
$X_0(n)$	$x(n), x(n-1), \cdots, x(n-N)$
$X_1(n)$	$\sin[\pi x(n)], \sin[\pi x(n-1)], ..., \sin[\pi x(n-N)]$
$X_2(n)$	$\cos[\pi x(n)], \cos[\pi x(n-1)], ..., \cos[\pi x(n-N)]$
$X_3(n)$	$\sin[2\pi x(n))], \sin[2\pi x(n-1)], ..., \sin[2\pi x(n-N)]$
$X_4(n)$	$\cos[2\pi x(n)], \cos[2\pi x(n-1)], ..., \cos[2\pi x(n-N)]$

TABLE 4. Channel input vectors in the EMFN filter.

Input vector	Elements
$X_0(n)$	$x(n), x(n-1), x(n-2), ..., x(n-N)$
$X_1(n)$	$\cos[\pi x(n)], \cos[\pi x(n-1)], ..., \cos[\pi x(n-N)]$
$X_2(n)$	$\sin[\pi x(n)/2]\sin[\pi x(n-1)/2], ...,$
	$\sin[\pi x(n-N+1)/2]\sin[\pi x(n-N)/2]$
...	...
$X_{N_2}(n)$	$\sin[\pi x(n)/2]\sin[\pi x(n-N_2+1)/2], ...$
$X_{N_2+1}(n)$	$\sin[3\pi x(n)/2], \sin[3\pi x(n-1)/2], ..., \sin[3\pi x(n-N)/2]$
$X_{N_2+2}(n)$	$\cos[\pi x(n)]\cos[\pi x(n-1)/2],$
	$..., \cos[\pi x(n-N+1)]\sin[\pi x(n-N)/2]$
...	...
$X_{N_2+1+P_3}(n)$	$\cos[\pi x(n)]\cos[\pi x(n-P_3)/2],$
	$\cos[\pi x(n-1)]\cos[\pi x(n-P_3-1)/2], ...$
$X_{N_2+2+P_3}(n)$	$\sin[\pi x(n)/2]\cos[\pi x(n-1)],$
	$..., \sin[\pi x(n-N+1)/2]\cos[\pi x(n-N)]$
...	...
$X_{N_2+1+2P_3}(n)$	$\sin[\pi x(n)/2]\cos[\pi x(n-P_3)],$
	$\sin[\pi x(n-1)/2]\cos[\pi x(n-P_3-1)]...$
$X_{N_2+2+2P_3}(n)$	$\sin[\pi x(n)/2]\sin[\pi x(n-1)/2]\sin[\pi x(n-2)/2],$
	$\sin[\pi x(n-1)/2]\sin[\pi x(n-2)/2]\sin[\pi x(n-3)/2], ...$
...	...
$X_{N_2+N_3}(n)$	$\sin[\pi x(n)/2]\sin[\pi x(n-P_3+1)/2]\sin[\pi x(n-P_3)/2],$
	$\sin[\pi x(n-1)/2]\sin[\pi x(n-P_3)/2]\sin[\pi x(n-P_3-1)/2], ...$

of P is given by

$$y(n) = f^T(W_0(n))X_0(n) + \sum_{k=1}^{M} f^T(W_k(n))X_k(n) \qquad (10)$$

where $M + 1 = 2P + 1$ and the channel input vectors are listed in Table 3.

C. EVEN FUNCTION NONLINEAR (EMFN) FILTER

The FLANN filter is constructed based on the expansion of the trigonometric basis. This expansion does not satisfy the Stone-Weierstrass theorem [14]. Thus, the FLANN filter cannot perfectly model nonlinear functions containing cross product terms, that is, the multiplication terms, with different time shift units, because the expansion of a FLANN basis function does not contain these cross terms.

TABLE 5. Multiplications in the sparse SEQ-RLS algorithm.

Items	Multiplications
$\sum_{k=0}^{M} X_k^T(n) f(W_k(n-1))$	$\sum_{j=0}^{M} s_j N_j$
$\alpha(n)$	None
$k_j(n)$	$\sum_{j=0}^{M} \{(s_j N_j)N_j + (s_j N_j)^2 + 2\}$
$Q_j(n)$	$\sum_{j=0}^{M} \{(s_j N_j)N_j + N_j^2 + 1\}$
$W_j(n)$	$\sum_{j=0}^{M} N_j$
$y(n)$	$\sum_{j=0}^{M} s_j N_j$
Total	$\sum_{j=0}^{M} \{(s_j+1)^2 N_j^2 + (2s_j+1)N_j + 3\}$
Total for $s_j = 1$	$\sum_{j=0}^{M} \{4N_j^2 + 3N_j + 3\}$
Standard RLS	$4N_T^2 + 3N_T + 3$; $N_T = \sum_{j=0}^{M} N_j$

In order to improve echo path modeling, an even-mirror Fourier nonlinear (EMFN) filter recently introduced [15] can be applied to approximate the input–output relationship of the nonlinear echo path. A third-order EMFN Filter system using the SEQ-RLS algorithm is proposed for NAEC applications. Table 4 lists the EMFN second- and third- order input vectors. Since the non-linear signal elements are bounded using the trigonometric functions, better filter properties will be expected.

D. COMPUTATIONAL COMPLEXITY

Let us denote s_j as the sparsity of channel j at time n, where the sparsity is defined as a ratio of the number of non-zero elements over the total number of elements in the diagonal channel. We can determine the numbers of multiplications and additions per iteration for a general sparse SEQ-RLS algorithm. The results are listed in Table 5 and Table 6, respectively. To simplify our comparisons, we omit the computation load for generating the first element of input signal in each diagonal channel. Therefore, both the Volterra and EMNF filters have the same computational complexity.

Note that the sparsity changes at the different channels and iterations. To simplify our analysis by setting $s_j = 1$ and applying results of the upper bounds listed in Table 5, we can derive the total number of multiplications per iteration for the third-order Volterra and EMFN filters as:

$$\begin{aligned}&\text{Number of multiplications (Volterra/EMFN)}\\ &= 3[4(N+1)^2 + 3(N+1) + 3]\\ &\quad + \sum_{j=1}^{N_2} [4(N+1-j)^2 + 3(N+1-j) + 3]\end{aligned}$$

TABLE 6. Additions in the sparse SEQ-RLS algorithm.

Items	Additions
$\sum_{k=0}^{M} X_k^T(n) f(W_k(n-1))$	$\sum_{j=0}^{M}(s_j N_j - 1)$
$\alpha(n)$	1
$k_j(n)$	$\sum_{j=0}^{M}\{(s_j N_j - 1)N_j + (s_j N_j - 1) + 1\}$
$Q_j(n)$	$\sum_{j=0}^{M}\{(s_j N_j - 1)N_j + N_j^2\}$
$W_j(n)$	$\sum_{j=0}^{M} N_j$
$y(n)$	$\sum_{j=0}^{M}(s_j N_j - 1)$
Total	$1 + \sum_{j=0}^{M}\{(2s_j + 1)N_j^2 + (3s_j - 1)N_j - 1\}$
Total for $s_j = 1$	$1 + \sum_{j=0}^{M}\{3N_j^2 + 2N_j - 1\}$
Standard RLS	$3N_T^2 + 2N_T$; $N_T = \sum_{j=0}^{M} N_j$

$$+2\sum_{j=1,P_3\geq 2}^{P_3}[4(N+1-j)^2+3(N+1-j)+3] + \sum_{j=1,P_3\geq 2}^{P_3}(j-1)[4(N+1-j)^2+3(N+1-j)+3]. \quad (11)$$

To calculate the total number of multiplications using the standard RLS algorithm (see Table 5.) for a comparison, we first determined the required total number of elements by

$$N_{T-VT/EMF} = 3(N+1)+\sum_{j=1}^{N_2}(N+1-j) + 2\sum_{j=1,P_3\geq 2}^{P_3}(N+1-j)+\sum_{j=1,P_3\geq 2}^{P_3}(j-1)(N+1-j). \quad (12)$$

And then the total number of multiplications can be determined using the formula on the last row in Table 5. For the FLANN filter, we can easily yield the computational load for multiplications as

$$\text{Number of multiplications} = (M+1)[4(N+1)^2+3(N+1)+3] \quad (13)$$

where $M+1 = 2P+1$ is the number of channels and P is the order of the FLANN filter. Given the total number of elements in the FLANN filter as

$$N_{T-FLANN} = (M+1)(N+1), \quad (14)$$

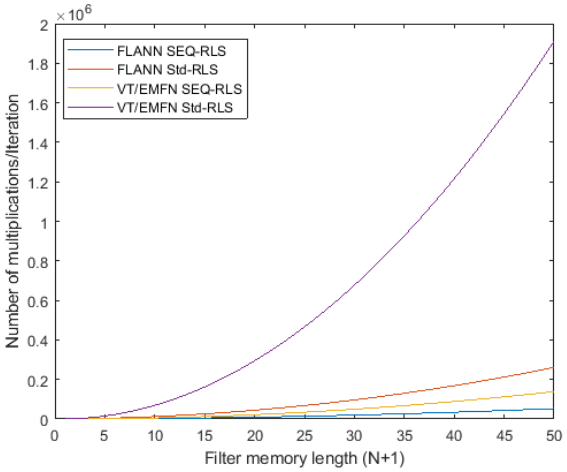

FIGURE 2. Number of multiplications per iteration versus the filter memory length with $s_j = 1$; for the Volterra filter (VT): $N_2 = 2$ and $P_3 = 3$; the FLAAN filter: $P = 2$; for the EMFN filter: $N_2 = 2$ and $P_3 = 3$.

we can determine the complexity of multiplications via Table 5. Fig. 2 depicts the multiplication complexity for each filter versus the filter memory length of $(N+1)$.

Again, using Table 6, the required additions for the Volterra/EMFN, and FLANN filters can be determined, respectively. The results are listed below.

$$\text{Number of additions (Volterra/EMFN)} = 1+3[3(N+1)^2+2(N+1)-1] + \sum_{j=1}^{N_2}[3(N+1-j)^2+2(N+1-j)-1] + 2\sum_{j=1,P_3\geq 2}^{P_3}[3(N+1-j)^2+2(N+1-j)-1] + \sum_{j=1,P_3\geq 2}^{P_3}(j-1)[3(N+1-j)^2+2(N+1-j)-1]. \quad (15)$$

$$\text{Number of additions (FLANN)} = 1+(M+1)[3(N+1)^2+2(N+1)-1]. \quad (16)$$

The number of additions for each of the standard RLS Volterra, EMFN, and FLANN filters can be determined using the result on the last row in Table 6, (12) and (14). Fig. 3 displays their comparisons.

From Figs. 2 and 3, we see that using the significant diagonal channels equipped with the SEQ-RLS algorithm can significantly reduce the computational load when the filter memory length increases. A further reduction of computation can be yielded when the sparsity factor is taken into account. It should be pointed out that introducing the sparsity may cause performance degradation if the threshold value ε in the discard function (6) is not properly chosen.

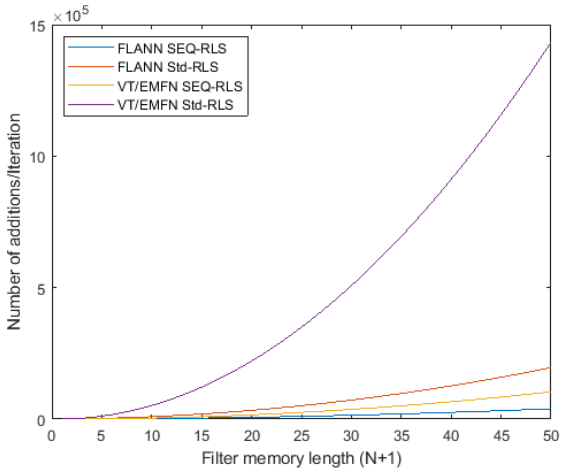

FIGURE 3. Number of additions per iteration versus the filter memory length with $s_j = 1$. For the Volterra filter (VT): $N_2 = 2$ and $P_3 = 3$; for the FLANN filter: $P = 2$; for the EMFN filter: $N_2 = 2$ and $P_3 = 3$.

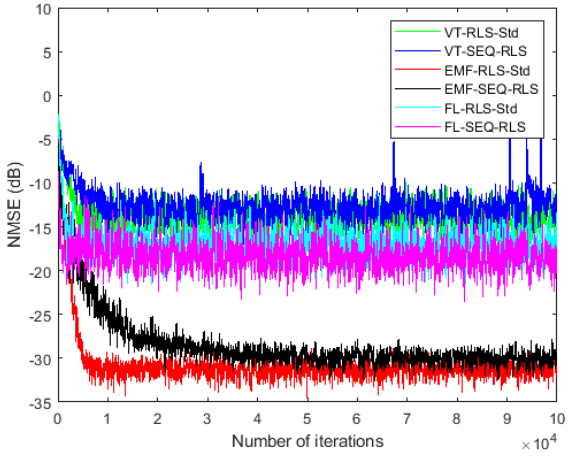

FIGURE 4. NMSE performance comparisons of system identification for (17) with the sparse sequential-RLS algorithms and standard function expansion RLS algorithms.

IV. COMPUTER SIMULATIONS

A. SYSTEM IDENTIFICATION

To validate the developed algorithms, we first perform nonlinear system identification and compare the performances with the Volterra, FLANN and EMFN adaptive filters each using the sparse SEQ-RLS algorithm respectively. Then we further investigate the effect of sparsity. To begin, two nonlinear systems which are assumed to present the nonlinear acoustic echo path are given in (17) and (18). The system expressed in (17) consists of the linear section and nonlinear section with products of delayed trigonometric elements. The second system is a typical polynomial systems with the cross product terms.

$$\begin{aligned} d(n) = {} & 0.3x(n-1) + 0.5x(n-3) - 0.4\cos[\pi x(n)] \\ & + \cos[\pi x(n-3)] - \sin[\pi x(n-1)/2]\sin[\pi x(n-2)/2] \\ & + \sin[3\pi x(n)/2] - 0.9\sin[3\pi x(n-2)/2] \\ & + 0.5\cos[\pi x(n)]\sin[\pi x(n-1)/2] \\ & - 0.6\sin[\pi x(n-1)/2]\cos[\pi x(n-3)] \\ & + \sin[\pi x(n-1)/2]\sin[\pi x(n-2)/2]\sin[\pi x(n-3)/2] \\ & + v(n); \end{aligned} \tag{17}$$

$$\begin{aligned} d(n) = {} & 0.3x(n-1) + 0.5x(n-3) - 0.4x^2(n) + x^2(n-3) \\ & - x(n-1)x(n-2) + x^3(n) - 0.9x^3(n-2) \\ & + 0.5x^2(n)x(n-1) - 0.6x(n-1)x^2(n-3) \\ & + x(n-1)x(n-2)x(n-3) + v(n). \end{aligned} \tag{18}$$

In (17) and (18), the input signal of $x(n)$ is the uniformly distributed white noise and $v(n)$ is the random noise which has a Gaussian distribution. The signal to noise power ratio (SNR) of 30 dB is used for all the simulations. Each adaptive filter with a memory size of $N + 1 = 10$ is adopted. We use the normalized mean square error (NMSE) for performance comparisons. The NMSE is assembled over 100 runs versus the number of iterations as defined below:

$$NMSE = 10\log_{10}\left(\frac{E\{e^2(n)\}}{\sigma_d^2}\right) \tag{19}$$

where σ_d^2 is the power of signal $d(n)$. For all the simulations, we use the following parameters for a fair comparison:

RLS algorithm:

$$\begin{aligned} & \lambda = 1 - 0.01/(N+1); \quad \delta = 0.01; \\ & Q_j(-1) = \delta I / E\{x_j^2(n)\}; \quad W_j(-1) = 0; \\ & j = 0, 1, \ldots, M, \end{aligned}$$

where M is the number of diagonal channels while $E\{x_j^2(n)\}$ indicates the power of the time-invariant channel.

Volterra filter: $N_2 = 2$ and $P_3 = 3$;
FLANN filter: $P = 2$;
EMFN filter: $N_2 = 2$ and $P_3 = 3$;
Sparsity: $s_j = 1$

For the standard non sequential RLS algorithm:

$$\begin{aligned} & \lambda = 1 - 0.01/(N+1); \quad \delta = 0.01 \\ & Q(-1) = \delta I / \sum_j E\{x_j^2(n)\}; \quad W(-1) = 0; \end{aligned}$$

where $\sum_j E\{x_j^2(n)\}$ indicates the sum of powers from all the time-invariant channels.

Fig. 4 and Fig. 5 display the plots of NMSEs for the system in (17) and the system in (18), respectively. It can be seen that the EMFN filter with a sequential RLS algorithm is the best performing system for (17). This is due to the fact that (17) is a type of the EMFN model. The proposed EMFN filter's performance is close to the standard EMFN RLS algorithm. The Volterra filter with a sequential RLS algorithm performs the best for identifying the system expressed in (18). Note that (18) is a type of the Volterra model and the performance from the proposed Volterra filter achieves the same level as

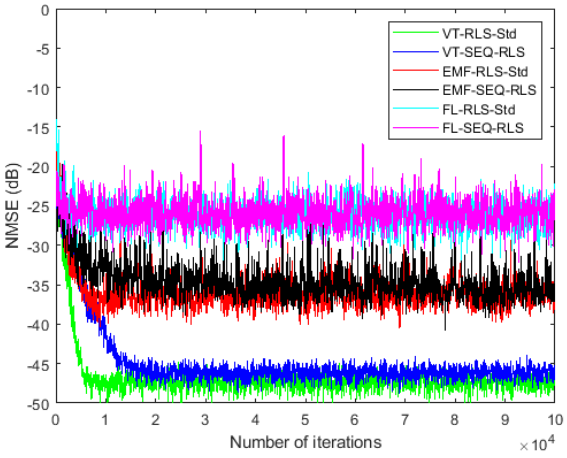

FIGURE 5. NMSE performance comparisons of system identification for (18) with the sparse sequential-RLS algorithms and standard function expansion RLS algorithms.

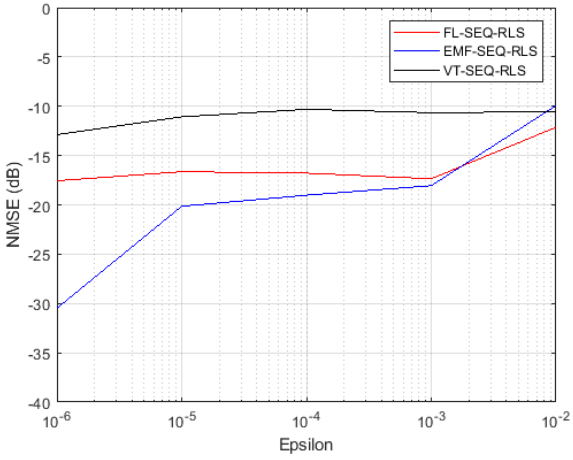

FIGURE 6. NMSE versus ε (threshold in the discard function) for the RLS based algorithms for (17).

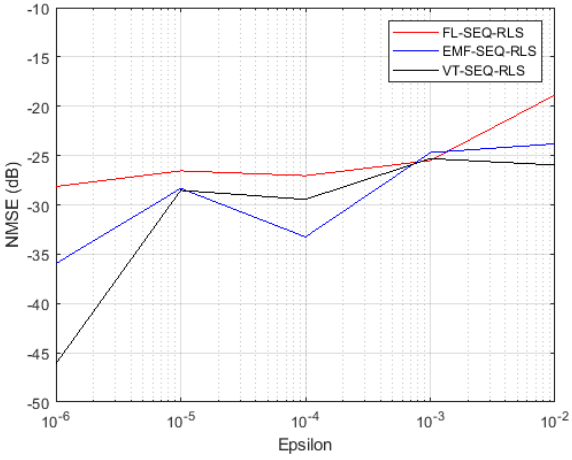

FIGURE 7. NMSE versus ε (threshold in the discard function) for the RLS based algorithms for (18).

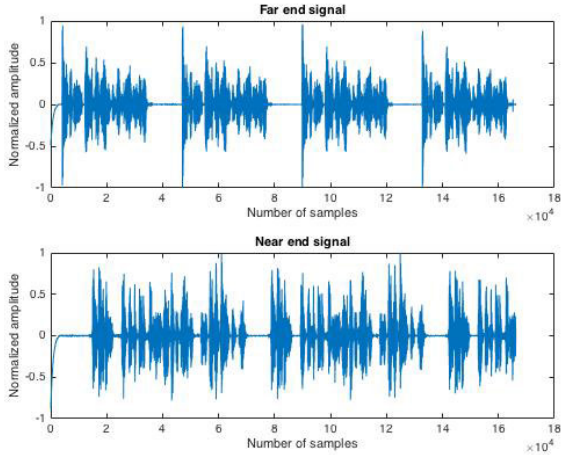

FIGURE 8. Speech signal used in the simulations (Fs=8000 Hz).

that from the standard RLS Volterra filter. Clearly, the effectiveness of using the function expansion filters depends on the system model. Next, the sparsity effect in these two systems is investigated by plotting the NMSE versus various values of ε (threshold value for the discard function) ranging from 0.000001 to 0.01, as shown in Fig. 6 for (17) and Fig. 7 for (18). As shown in Fig. 6, it is evident that the EMFN filter is more sensitive to the threshold value since the system model is an EMFN type.

A similar trend can be seen in the NMSE performance comparison as shown in Fig. 7 for the system given in (18). Since the system model is a Volterra type model, the Volterra filter is more sensitive to the threshold value.

For effective system identification, that is, the EMFN filter for (17) and the Volterra filter for (18), under the 30 dB noisy environment, the performance will significantly suffer if the sparsity is emphasized during the implementation, that is, $\varepsilon > 0.00001$. This result suggests that in the noisy environment condition, the discard function is not preferred unless further reduction of computational load is a must.

B. SINGLE TALK SIMULATIONS

For the application of nonlinear echo cancellation, we adopt the far end and near end speech segments with a sampling rate of 8000 Hz shown in Fig. 8.

The nonlinear echo path consists of the nonlinear function cascaded by a linear acoustic impulse response (AIR) echo path shown in Fig. 9, which is a 150th order polynomial model extracted from the AIR multichannel impulse response database [21], [22]. The memoryless nonlinearity is introduced before the linear echo path model, which is a piecewise nonlinear system defined below:

$$f(x) = \begin{cases} 2x/(3\xi) & |x| \le \xi \\ sign(x)\left(3-(2-|x/\xi|)^2\right)/3\right) & \xi < |x| \le 2\xi \\ sign(x) & 2\xi < |x| \le 1 \end{cases} \quad (20)$$

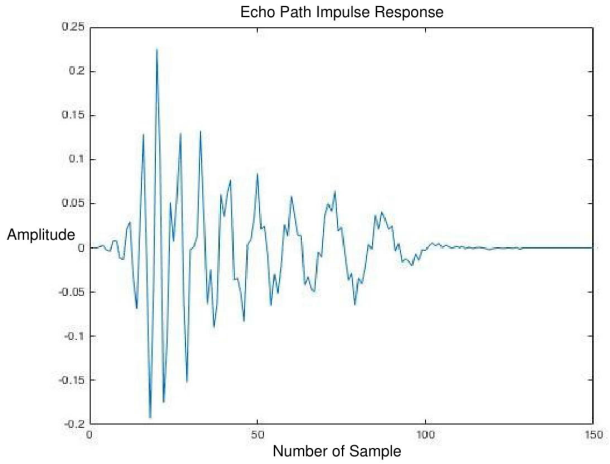

FIGURE 9. Echo cancellation path (FIR model).

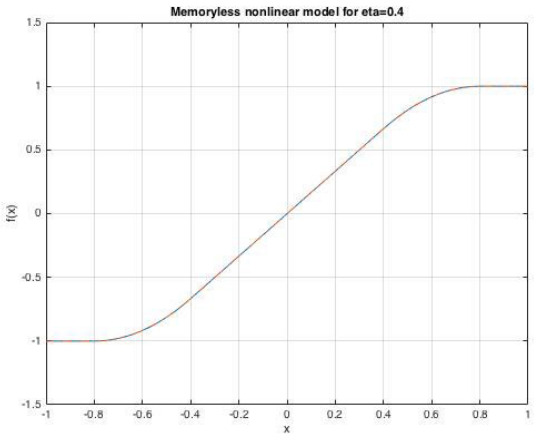

FIGURE 10. Input and output of the nonlinear system.

where ξ is the controlling factor and set to 0.4. The system input and output relation is depicted in Fig. 10.

For a nonlinear adaptive filter to effectively model the specified echo path, a filter memory length of $(N+1) = 150$ must be chosen to cover the time response. This filter memory size hinders real-time application (even off-line simulations) if a standard function expansion RLS algorithm is used. For the third-order Volterra or EMF filter, the total number of filter coefficients [7] can reach $(N+1+3)!/[(N+1)!3!] - 1 = 153!/(150!3!) - 1 = 589151$. Matrix $Q(n)$ will then have a size of 589151×589151. Therefore, we only conduct simulations for the proposed sequential RLS algorithms. Again, to reduce the effect of initial condition and have a fair comparison, the same parameters for the RLS algorithm setup for Volterra, FLANN and EMFN filters are used and listed below:

$$
\begin{aligned}
&N = 149;\\
&\lambda = 1 - 0.01/(N+1); \quad \delta = 0.0001\\
&Q_j(-1) = \delta I/E\{x_j^2(n)\};\\
&W_j(-1) = 0, \text{ and } s_j = 1;\\
&\text{Volterra filter: } N_2 = 3 \text{ and } P_3 = 2;
\end{aligned}
$$

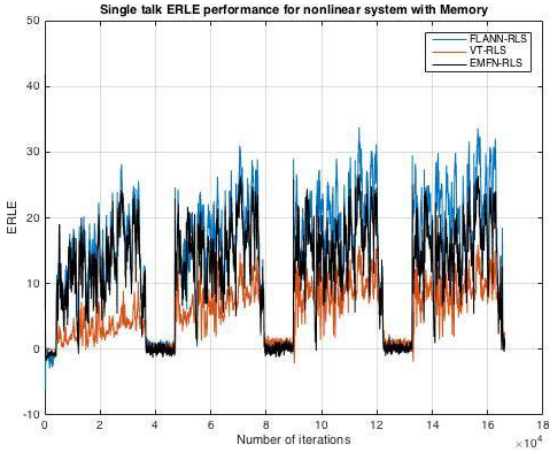

FIGURE 11. ERLE performance comparisons of single talk scenario.

$$
\begin{aligned}
&\text{FLANN filter: } P = 2;\\
&\text{EMFN filter: } N_2 = 3 \text{ and } P_3 = 2.
\end{aligned}
$$

To validate the performance of echo cancellation, a standard criterion of the echo return loss enhancement (ERLE), which is the ratio of send-in signal power and the residue signal power after the cancellation, assembled over 100 runs versus the number of iterations, is used:

$$ERLE\ dB = 10\log_{10}\left(\frac{E\{y^2(n)\}}{E\{e^2(n)\}}\right). \tag{21}$$

Note that $y(n)$ is the echo to be cancelled while $e(n)$ is the residual signal after nonlinear echo cancellation.

In our single talk scenario, a SNR of 30 dB is assumed at the near end for simulations. The performances of ERLEs from all three algorithms are obtained and displayed in Fig. 11, respectively. As shown in Fig. 11, the FLANN canceler achieves the highest ERLE value while the Volterra canceler has the lowest ERLE value. The performance of echo cancellation from the EMFN canceler is close to the one from the FLANN canceller. This can explained as follows: the nonlinear acoustic echo path is assumed to have a memoryless saturation model cascaded by the linear time invariant system. The resultant nonlinear system may not contain the cross-product terms. Therefore, the FLANN filter has a better match to the echo path. The EMFN filter can also match well but wastes the trigonometric product terms. The Volterra filter cannot compete with the other two methods due to the fact that many cross-product terms cannot take effect.

C. DOUBLE TALK SIMULATIONS

In this simulation, we repeat the previous experiments by using the same echo path in a double talk situation. The parameter settings are listed below.

$$
\begin{aligned}
&N = 149;\\
&\lambda = 1 - 0.01/(N+1); \quad \delta = 0.0001\\
&Q_j(-1) = \delta I/E\{x_j^2(n)\};\\
&W_j(-1) = 0, \text{ and } s_j = 1;
\end{aligned}
$$

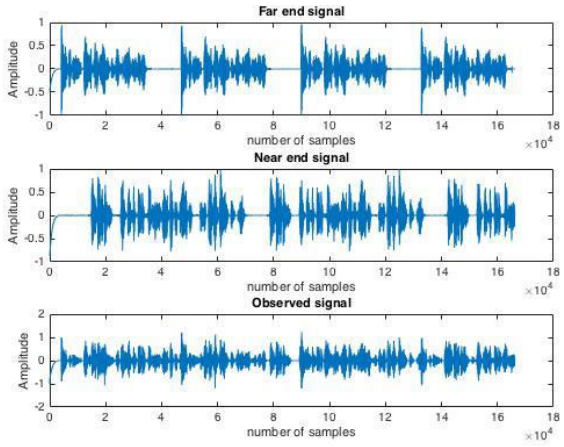

FIGURE 12. Far end, near end and observed signals for the nonlinear ACE.

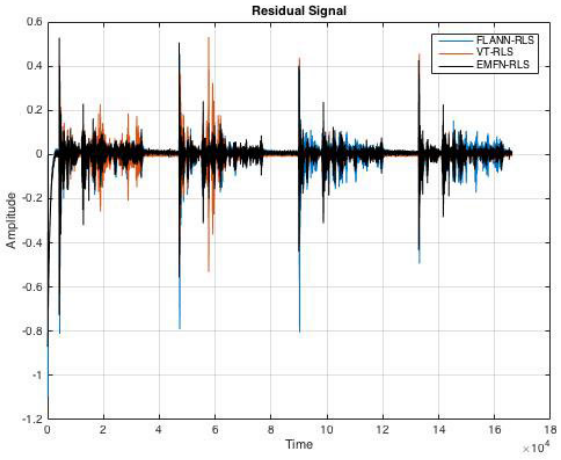

FIGURE 13. Residual signals from the memoryless system.

$$\text{Volterra filter: } N_2 = 2 \text{ and } P_3 = 3;$$
$$\text{FLANN filter: } P = 2;$$
$$\text{EMFN filter: } N_2 = 2 \text{ and } P_3 = 3.$$

Notice that both the Volterra and EMFN filters use 3 diagonal channels for the second-term terms and 10 diagonal channels for the third-order terms, respectively. The FLANN filter has 5 time invariant channels.

To evaluate the performance for the case of a double talk scenario, the ERLE measurement is not appropriate since the near end speech creates residue power which disturbs the measurement. Instead, the residue signal, that is, $e(n) - s(n)$, which is the difference between the echo cancelled signal $[s(n)+d(n)-y(n)]$ and the near end signal $(s(n))$ is examined, where $d(n)$ is the echo signal due to the far end speech appearing at the near end. Fig. 12 depicts the far end, near end and observed signals (echo+near end signal).

After nonlinear echo cancellation, according to the plotted residual signals, the method which gives the minimum amplitudes is the best performing NAEC system for the double talk scenario. Fig. 13 demonstrates the performances. From the residual signal plot in Fig. 13, it can be noted that the EMFN filter achieves lower amplitudes than the other two filters. The Volterra filter catches the echo cancellation quality after it converges. This may be due to that when the near end speech signal is involved in the nonlinear acoustic echo cancellation, the cross-terms from both EMFN and Voltera filters take an effect. As a conclusion, the EMFN filter shows its advantage for both single talk and double talk scenarios.

V. CONCLUSION

We have developed the function expansion adaptive filters by applying the sparse SEQ-RLS algorithm for nonlinear acoustic echo cancellation. The algorithm is developed based on a diagonal channel structure from the Volterra filter and updating dominant coefficients with consideration of sparse elements in the diagonal channel. The third-order Volterra, third-order even mirror Fourier nonlinear (EMFN), and functional link artificial neural network (FLANN) filters are developed according to the sparse SEQ-RLS algorithm. The computation complexity for each filter algorithm is analyzed. From the performance of nonlinear echo cancellation in single and double talk scenarios, all proposed function expansion filters equipped with the sparse SEQ-RLS algorithm are effective for nonlinear echo cancellation. In general, the EMFN filter provides better performance in comparison with the other functional expansion filters.

REFERENCES

[1] L. Tan and J. Jiang, *Digital Signal Processing: Fundamentals and Applications*, 3rd Ed. Amsterdam, The Netherlands: Elsevier, 2018.

[2] A. Stenger, L. Trautmann, and R. Rabenstein, "Nonlinear acoustic echo cancellation with 2nd order adaptive Volterra filters," in *Proc. IEEE Int. Conf. Acoust., Speech, Signal Process.*, Phoenix, AZ, USA, Mar. 1999, pp. 877–880.

[3] A. Guerin, G. Faucon, and R. L. Bouquin-Jeannes, "Nonlinear acoustic echo cancellation based on Volterra filters," *IEEE Trans. Speech Audio Process.*, vol. 11, no. 6, pp. 672–683, Nov. 2003.

[4] D. Comminiello, M. Scarpiniti, L. A. Azpicueta-Ruiz, J. Arenas-Garcia, and A. Uncini, "Full proportionate functional link adaptive filters for nonlinear acoustic echo cancellation," in *Proc. 25th Eur. Signal Process. Conf. (EUSIPCO)*, Kos, Greece, Aug. 2017, pp. 1145–1149.

[5] D. Comminiello, M. Scarpiniti, L. A. Azpicueta-Ruiz, J. Arenas-García, and A. Uncini, "Nonlinear acoustic echo cancellation based on sparse functional link representations," *IEEE/ACM Trans. Audio, Speech, Language Process.*, vol. 22, no. 7, pp. 1172–1183, Jul. 2014.

[6] Y. Huang, J. Skoglund, and A. Luebs, "Practically efficient nonlinear acoustic echo cancellers using cascaded block RLS and FLMS adaptive filters," in *Proc. IEEE Int. Conf. Acoust., Speech Signal Process. (ICASSP)*, New Orleans, LA, USA, Mar. 2017, pp. 597–600.

[7] L. Tan and J. Jiang, "Adaptive Volterra filters for active control of nonlinear noise processes," *IEEE Trans. Signal Process.*, vol. 49, no. 8, pp. 1667–1676, Aug. 2001.

[8] D. P. Das and G. Panda, "Active mitigation of nonlinear noise processes using a novel filtered-s LMS algorithm," *IEEE Trans. Speech Audio Process.*, vol. 12, no. 3, pp. 313–322, May 2004.

[9] L. Tan, V. Vijayarajan, N. M. Chimitt, J. Jiang, and A. Togbe, "Channel sparsity-aware recursive least squares algorithms for nonlinear system modeling and active noise control," in *Proc. IEEE 8th Annu. Ubiquitous Comput., Electron. Mobile Commun. Conf. (UEMCON)*. New York, NY, USA: Columbia Univ., Oct. 2017, pp. 225–231.

[10] V. Vijavarajan, J. Dai, L. Tan, and J. Jiang, "Channel sparsity-aware diagonal structure Volterra filters for nonlinear acoustic echo cancellation," in *Proc. IEEE Int. Conf. Electro/Inf. Technol. (EIT)*. Rochester, MI, USA: Oakland Univ., May 2018, pp. 420–423.

[11] L. Tan and J. Jiang, "Adaptive second-order Volterra filtered-X RLS algorithms with sequential and partial updates for nonlinear active noise control," in *Proc. 4th IEEE Conf. Ind. Electron. Appl.*, Xian, China, May 2009, pp. 1625–1630.

[12] L. Tan, "Adaptive function expansion RLS filters with dynamic selection of channel updates for nonlinear active noise control," in *Proc. Int. Conf. Intell. Control Inf. Process.*, vol. 2, Dalian, China, Aug. 2010, pp. 1–6.
[13] L. Tan and J. Jiang, "Adaptive second-order Volterra RLS algorithms with dynamic selection of channel updates," in *Proc. IEEE/ASME Int. Conf. Adv. Intell. Mechatronics*, Montreal, QC, Canada, Jul. 2010, pp. 1323–1328.
[14] A. Carini and G. L. Sicuranza, "Perfect periodic sequences for even mirror Fourier nonlinear filters," *Signal Process.*, vol. 104, pp. 80–93, Nov. 2014.
[15] X. Guo, C. Dong, L. Tan, and S. Du, "Adaptive even mirror Fourier filtered error LMS algorithm for multichannel nonlinear active noise control," in *Proc. IEEE 7th Annu. Inf. Technol., Electron. Mobile Commun. Conf. (IEMCON)*, Oct. 2016, pp. 1–6.
[16] X. Guo, Y. Li, J. Jiang, C. Dong, S. Du, and L. Tan, "Sparse modeling of nonlinear secondary path for nonlinear active noise control," *IEEE Trans. Instrum. Meas.*, vol. 67, no. 3, pp. 482–496, Mar. 2018.
[17] L. Tan and J. Jiang, "An adaptive technique for modeling second-order Volterra systems with sparse kernels," *IEEE Trans. Circuits Syst. II, Analog Digit. Signal Process.*, vol. 45, no. 12, pp. 1610–1615, Dec. 1998.
[18] L. Z. Tan and J. Jiang, "Adaptive second-order Volterra delay filter," *Electron. Lett.*, vol. 32, no. 9, pp. 807–809, Apr. 1996.
[19] Y. Chen, Y. Gu, and A. O. Hero, "Sparse LMS for system identification," in *Proc. IEEE Int. Conf. Acoust., Speech Signal Process.*, Taipei, Taiwan, Apr. 2009, pp. 3125–3128.
[20] H. Yazdanpanah and P. S. R. Diniz, "Recursive least-squares algorithms for sparse system modeling," in *Proc. IEEE Int. Conf. Acoust., Speech Signal Process. (ICASSP)*, New Orleans, LA, USA, Mar. 2017, pp. 3879–3883.
[21] Rwth Aachen University (Germany) and Bar-Ilan Uni-versity (Israel). (2014). *Multichannel Impulse Response Database*. Accessed: Sep. 16, 2015. [Online]. Available: http://http://www.ind.rwth-aachen.de/en/research/tools-downloads/multichannel-impulse-response-database/
[22] *Digital Network Echo Cancellers*, Standard ITU-T Rec. G.168, 2002.

JEAN JIANG (Senior Member, IEEE) received the B.S. and M.S. degrees in electrical engineering from Southeast University, Nanjing, China, in 1982 and 1985, respectively, and the Ph.D. degree in electrical engineering from The University of New Mexico, Albuquerque, NM, USA, in 1992.

She is currently an Associate Professor with the College of Technology, Purdue University Northwest, Hammond, IN, USA. She has authored or coauthored two textbooks *Digital Signal Processing: Fundamentals and Applications* (Elsevier, Third Edition, 2018) and *Analog Signal Processing and Filter Design* (Linus Publications, Second Edition, 2016). Her research interests include digital signal processing, adaptive signal processing, control systems, computer vision, and robotics.

VINITH VIJAYARAJAN was born in Madurai, India. He received the Bachelor of Engineering (B.E.) degree in electronics and communication engineering from the Mepco Schlenk Engineering College, Sivakasi, India, in 2016, and the M.S. degree in electrical engineering from Purdue University Northwest, Hammond, IN, USA, in 2018.

He is currently an Audio-Voice T-Development Engineer with Qualcomm Inc., San Diego, CA, USA. His research interests include digital signal processing, adaptive signal processing, ambisonics, and audio QOS testing.

LIZHE TAN (Senior Member, IEEE) received the B.S. degree from Southeast University, Nanjing, China, in 1984, and the M.S. degree in engineering mechanics and the M.S. and Ph.D. degrees in electrical engineering from The University of New Mexico, Albuquerque, NM, USA, in 1987, 1989, and 1992, respectively.

He is currently a Professor with the Department of Electrical and Computer Engineering, Purdue University Northwest, Hammond, IN, USA. He has authored or coauthored two textbooks *Digital Signal Processing: Fundamentals and Applications* (Elsevier, Third Edition, 2018) and *Analog Signal Processing and Filter Design* (Linus Publications, Second Edition, 2016). He holds a granted U.S. patent. His research interests include digital signal processing, adaptive signal processing, control systems, computer vision, and robotics. He has served as an Associate Editor for the *International Journal of Engineering Research and Innovation*.